Granular Matter (2005) 7: 185–190
DOI 10.1007/s10035-005-0210-5

ORIGINAL PAPER

Linda Djaoui · Jérôme Crassous

Probing creep motion in granular materials with light scattering

Received: 9 November 2004 / Published online: 12 August 2005

Abstract We describe a dynamic light scattering experiment designed in order to study creep motion in granular materials. This method is based on the recording of the speckle pattern with a charge coupled device (CCD) camera. The autocorrelation function of the scattered electric field is calculated and related to the displacement field of the beads. As an application, the measurement of the thermal expansion of a granular material subjected to temperature variations is presented.

Keywords Creep motion · Deformation and plasticity · Diffusive light scattering

1 Introduction

The dynamics of granular materials under shear stresses play an important role in many natural phenomena and technological applications. From an ideal point of view, when the shear stress exceeds a certain threshold, the granular material undergoes a transition from a frozen state to a fluidized state. Even if such a definition of two well defined states provides a rough description for many practical situations, no sharp transition between those two states of granular materials exists [1,2]. Indeed, careful experiments have shown that even if a granular material appears as a static solid, slow creeping motion takes place within, and no clear distinctions may be made between frozen and flowing states [3]. It has been suggested that such creep motion is a consequence of thermally activated processes where particles trapped in some metastable configuration escape due to energy fluctuations [2]. However, the thermal fluctuations are not large enough to overcome such barriers. The energy must be found elsewhere, as from stress fluctuations arising from the macroscopic flow itself or from external environment such as mechanical vibrations. The origin of creep motion, its amplitude or its possible localization are still controversial. A part of this difficulty lies in the fact that the measurement of the displacement field of amplitude as small as the scale of a grain is a difficult task, especially in an opaque system. Among the possible probes for such studies, light scattering appears as a particularly promising one. The basic idea is to observe the evolution of the speckle pattern arising from the light scattered by a granular medium during the motion of grains. Such kinds of measurements have already been performed on "gaseous" granular media flowing in a vertical pipe [4], and fluidized grain layer [5,6]. More recently, the reorganizations in an immersed granular medium induced by mechanical tapping have been investigated [7]. Such studies have shown that random motion at the scale of optical wavelengths may be probed by light scattering. We show here that light scattering may also be a convenient way to study continuous displacement fields within a granular medium. In the following section, we describe the optical set-up, the data acquisition and the data analysis. In section 3, we discuss the relation between the autocorrelation function of the electric field and the displacement field within the granular medium. This method is illustrated with the measurement of the thermal dilatation of a granular medium subjected to temperature variations in section 4.

L. Djaoui (✉) · J. Crassous
Laboratoire de Physique
École Normale Supérieure de Lyon
46 allée d'Italie, 69364 Lyon Cedex 07, France
E-mail: linda.djaoui@ens-lyon.fr
E-mail: jerome.crassous@ens-lyon.fr

2 Multispeckle light scattering

2.1 Background

We are interested in the measurement of slow creeping motion or reorganization occurring in granular media. Light scattering, as a probe for sensing particle displacements at the scale of optical wavelengths has already been successfully used. Durian used it previously for the measurement of velocity fluctuations in a granular gas flowing continuously [4]. In his experiment, the light scattered by the granular gas is analyzed by measuring the fluctuations of the intensity of light on a single coherence area. The temporal autocorrelation

function of the scattered intensity is then measured by operating a time average, and gives access to the mean square displacement of the particles. As pointed out by Viasnoff [8], such a set-up relies on the fact that the system evolution is stationary on the time scale of the experiment. Since we are interested in studying creeping motion or reorganization, such a technique is not suitable for our problem. The use of a charge coupled device (CCD) camera as a light sensor is a convenient way to tackle this issue [8,9] in both single and multiple scattering modes. The principle is to record simultaneously the intensity fluctuations on many different coherence areas. Different speckle spots evolve independently from each other, but all of them provide the same averaged information on the dynamics of the medium. Thus, one single image consists of a large number of independent samples. As a consequence, it is possible to measure, as a function of time, the temporal autocorrelation function of the scattered light with an excellent statistical accuracy. The disavantages of this method are the low sampling rate and the low sensitivity of the CCD sensors. Since we deal with slow evolution and highly diffusive materials, these limitations are not relevant for the study of creeping motion in a granular medium.

2.2 Experimental set-up

Figure 1 shows a schematic drawing of the experimental set-up in the transmission geometry. The samples consist of a glass cell filled with spherical glass beads. This cell is set inside a thermal enclosure which is stabilized to a fixed temperature with a typical 0.01 °C stability. The cell is illuminated with a 1.5 mW polarized HeNe laser (Melles Griot 05STP903) operating at $\lambda = 633$ nm. The laser beam is first expanded up to a diameter of a few millimeters. This permits the illumination of a wide area and allows physical quantities to be averaged over a large number of beads. The incident light is scattered by the granular medium, and is collected after a diaphragm, which is placed on the beam axis. A polarizer is placed perpendicular to the incident polarization to collect light which has been multiply scattered only. The light is then detected with a Cohu CCD camera model 4910, which is set approximatively 20 cm behind the diaphragm. The whole experiment is placed on an optical breadboard on a vibration isolated table. A simple wood box encloses the experiment in order to minimize external stray light. Images are collected using Scion's VG-5 frame grabber and they are encoded as 8-bit integer arrays $I_{raw}(p,t)$, representing the raw intensity at time t on the pixel p. These raw data are then corrected for noise contributions in order to determine the electric field autocorrelation function.

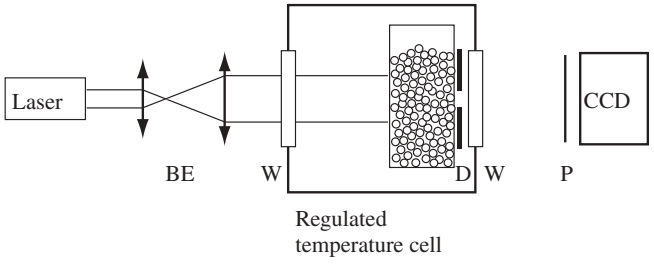

Fig. 1 Experimental set-up for recording light multiply diffused by a granular medium. BE : Beam Expander, W : Optical Window, D : Diaphragm, P : Dichroic polarizer

2.3 Correlation function calculation.

As will be explained in section 3, the relevant quantity for probing the motion of particles is the normalized electric field autocorrelation function

$$g_E(t_1,t_2) = \frac{< E_s(t_1)\cdot E_s^*(t_2) >}{< |E_s(t_1)| >< |E_s(t_2)| >} \quad (1)$$

where E_s is the scattered electric field, and the brackets $< \ldots >$ are an average over the speckle spots. The denominator on the right hand side of equation (1) involves both the electric field scattered at times t_1 and t_2. This normalization has the effect of correcting small changes in laser intensity [10]. When the scattered electric fields are Gaussian distributed, $|g_E(t_1,t_2)|$ is related to the intensity autocorrelation of the scattered intensity I_s by the Siegert relation [11]

$$\frac{< I_s(t_1)\cdot I_s(t_2) >}{< I_s(t_1) >< I_s(t_2) >} = 1 + \beta|g_E(t_1,t_2)|^2 \quad (2)$$

where β is a positive experimental factor of the order of unity. The raw experimental data $I_{raw}(p,t)$ are corrected for the effects of the camera dark noise and stray light and the factor β is determined in order to extract the relevant quantity $|g_E(t_1,t_2)|$. Our analysis of raw data is based on the fact that the raw intensity at time t on pixel p is the sum of the scattered intensity $I_s(p,t)$, the stray light $I_{str}(p,t)$ and the dark noise $I_{dn}(p,t)$ of the CCD sensor:

$$I_{raw}(p,t) = I_s(p,t) + I_{str}(p,t) + I_{dn}(p,t). \quad (3)$$

We moreover assume that the scattered light, stray light and sensor dark noise are independent and thus uncorrelated quantities

$$< I_s\cdot I_{str} >=< I_s >< I_{str} > \quad (4)$$

$$< I_s\cdot I_{dn} >=< I_s >< I_{dn} > \quad (5)$$

$$< I_{dn}\cdot I_{str} >=< I_{dn} >< I_{str} > \quad (6)$$

Let us now introduce the quantities

$$G_{raw}(t_1,t_2) =< I_{raw}(t_1)\cdot I_{raw}(t_2) > - < I_{raw}(t_1) >< I_{raw}(t_2) > \quad (7)$$

$$G_s(t_1,t_2) =< I_s(t_1)\cdot I_s(t_2) > - < I_s(t_1) >< I_s(t_2) > \quad (8)$$

$$G_{dn}(t_1,t_2) =< I_{dn}(t_1)\cdot I_{dn}(t_2) > - < I_{dn}(t_1) >< I_{dn}(t_2) > \quad (9)$$

$$G_{str}(t_1,t_2) =< I_{str}(t_1)\cdot I_{str}(t_2) > - < I_{str}(t_1) >< I_{str}(t_2) > \quad (10)$$

It follows from the absence of correlations between the different contributions to the raw intensity that:

$$G_{raw}(t_1,t_2) = G_s(t_1,t_2) + G_{dn}(t_1,t_2) + G_{str}(t_1,t_2) \quad (11)$$

The contribution $G_{dn}(t_1, t_2)$ from the dark noise of the camera is measured with the CCD shutter closed. It is found that the the dark noise is:

$$G_{dn}(t_1, t_2) = \sigma_{dn}^2 \delta(t_2 - t_1) \tag{12}$$

with σ_{dn} independent of time and $\delta(t_2 - t_1) = 1$ if $t_1 = t_2$, and 0 otherwise. The quantity σ_{dn} may also be determined by computing the difference $G_{raw}(t_1, t_1 + \Delta t) - G_{raw}(t_1, t_1)$, with Δt small compared to the evolution time of the scattered intensity. It follows that $G_s(t_1, t_1 + \Delta t) \approx G_s(t_1, t_1)$ and that $G_{raw}(t_1, t_1 + \Delta t) - G_{raw}(t_1, t_1) = \sigma_{dn}^2$.

The contribution $G_{str}(t_1, t_2)$ comes from a non uniform distribution of stray light. This quantity is determined by measuring the correlation between images corresponding to well uncorrelated scattered intensities, as occurs when granular media are shaken. Since the dark noise and the scattered intensity do not contribute to correlations of raw intensity, we measure only the contribution of stray intensity. It is found that:

$$G_{str}(t_1, t_2) = \sigma_{str}^2 \tag{13}$$

where σ_{str} does not depend in practice on times t_1 or t_2.

It follows directly from (11) that the correlation function may be determined as:

$$G_s(t_1, t_2) = G_{raw}(t_1, t_2) - \sigma_{str}^2 - \sigma_{dn}^2 \delta(t_2 - t_1) \tag{14}$$

Since the coherence factor β does not evolve with time, the normalized correlation function of the electric field $|g_E(t_1, t_2)|$ may be determined as:

$$|g_E(t_1, t_2)|^2 = \frac{G_s(t_1, t_2)}{\sqrt{G_s(t_2, t_2) \cdot G_s(t_1, t_1)}} \tag{15}$$

In the preceeding discussion dealing with the different contributions to noise, we did not explicitly distinguish the autocorrelation functions from their estimates on a finite number of speckle spots. Indeed, the finite number of speckle spots is responsible for statistical noise in the determination of the correlation function. The size s of the speckle spots of the scattered light is given by $s \approx d\lambda/a$, where d is the distance between the diaphragm and the camera, λ the laser wavelength, and a the diameter of the diaphragm. Thus, the number of coherence areas may be increased by decreasing the ratio d/a. However, when the coherence area becomes of the order of one pixel, the overlapping of different speckle spots on one pixel decreases the contrast of the speckle pattern. In practice, we find that a speckle spot spreading on 3 pixels is a good compromise between contrast and statistics.

3 Theory

The relation between the correlation function of the scattered electric field $g_E(t_1, t_2)$ and the displacement field of the beads composing the granular medium between the time t_1 and t_2 is computed by assuming that the light is multiply scattered by the random distribution of beads, and hence executes a random walk from bead to bead through the sample. In the weak scattering limit ($kl >> 1$, where k is the wave number, and l the scattering mean free path), and in the multiply scattering limit ($L >> l$, L being the thickness of the cell), the intensity of the light can be described by the diffusion approximation [12]. The autocorrelation function is then given by [13, 14]:

$$g_E(t_1, t_2) = \sum_{n=1}^{\infty} P(n) < \exp(j(\Phi_n(t_2) - \Phi_n(t_1))) > \tag{16}$$

where $P(n)$ is the fraction of the total scattered intensity in the light paths involving n scattering events. This quantity is related to the geometry of the experiment. The quantity $\Phi_n(t_2) - \Phi_n(t_1)$ is the phase difference of the scattered electric field between the time t_1 and t_2, associated with a given path involving n scattering events. The average $< ... >$ is calculated over all the paths involving n scattering events.

Figure 2 is a simplified geometrical view of the random walk of a photon across the different beads, composed of travels across beads, intersticial media, and refraction or reflection. Any displacement of matter will contribute to a variation of the optical length between t_1 and t_2. This could include not only the displacement of the centers $\mathbf{r}_\nu$ of the spheres, but also rotations of nonspherical beads or deformations of the beads. For the sake of simplicity, we will ignore such effects in the following discussions, although they are not expected to be systematically negligible. It follows from such simplifying assumptions that phase variations are:

$$\Delta\Phi_n = \gamma \cdot \Delta\Big[\sum_{\nu=1}^{\nu=n} \mathbf{k}_\nu \cdot (\mathbf{r}_{\nu+1} - \mathbf{r}_\nu)\Big] \tag{17}$$

where $\mathbf{k}_\nu = k.\mathbf{e}_\nu$ with k the wave number and $\mathbf{e}_\nu$ the unit vector parallel to $\mathbf{r}_{\nu+1} - \mathbf{r}_\nu$. The quantity γ is a numerical factor of the order of unity, which takes into account the fact that the optical ray joining the beads ν and $\nu + 1$ is not parallel to $(\mathbf{r}_{\nu+1} - \mathbf{r}_\nu)$. We will ignore this effect in the following and let $\gamma \approx 1$. Within this simplified framework, the phase shift between the times t_1 and t_2 may be written as:

$$\Delta\Phi_n = \sum_{\nu=1}^{\nu=n} \mathbf{k}_\nu(t_2) \cdot \big[\mathbf{r}_{\nu+1}(t_2) - \mathbf{r}_\nu(t_2)\big] - \sum_{\nu=1}^{\nu=n} \mathbf{k}_\nu(t_1) \cdot \big[\mathbf{r}_{\nu+1}(t_1) - \mathbf{r}_\nu(t_1)\big] \tag{18}$$

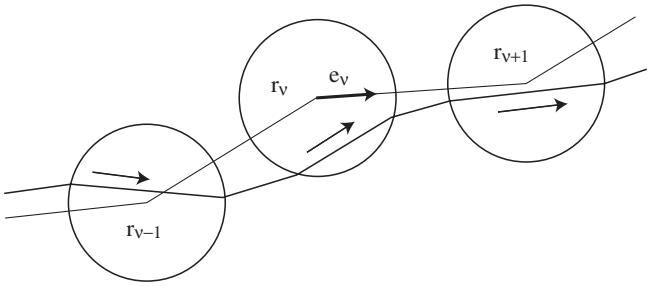

Fig. 2 Schematic view of a light ray consisting of numerous refractions propagating through the granular medium

Since $(\mathbf{k}_\nu(t_2) - \mathbf{k}_\nu(t_1)) \perp (\mathbf{r}_{\nu+1} - \mathbf{r}_\nu)$, we obtain:

$$\Delta\Phi_n = \sum_{\nu=1}^{\nu=n} \mathbf{k}_\nu \cdot \left[\mathbf{u}(\mathbf{r}_{\nu+1}) - \mathbf{u}(\mathbf{r}_\nu)\right] \tag{19}$$

where we have introduced the displacement field $\mathbf{u}(\mathbf{r})$ between the times t_1 and t_2. Equation (19) is indeed the expression of the phase shift previously derived for the analysis of Diffusing Wave Spectroscopy involving stationary flows of colloidal particles in a suspension [15–17]. For displacement fields which vary slowly on the scale of the bead size, we can expand the displacement field:

$$\begin{aligned}\mathbf{u}(\mathbf{r}_{\nu+1}) &= \mathbf{u}(\mathbf{r}_\nu + l_\nu.\mathbf{e}_\nu) \\ &\approx \mathbf{u}(\mathbf{r}_\nu) + l_\nu(\mathbf{e}_\nu \cdot \nabla)\mathbf{u}(\mathbf{r}_\nu)\end{aligned} \tag{20}$$

with $l_\nu = \|\mathbf{r}_{\nu+1} - \mathbf{r}_\nu\|$. It follows from equation (20) that:

$$\Delta\Phi_n = k \sum_{\nu=1}^{\nu=n} l_\nu \sum_{i,j} e_{\nu,i} e_{\nu,j} U_{ij}(\mathbf{r}_\nu) \tag{21}$$

where $i, j = x, y, z$, and $U_{ij} = (1/2)(\partial U_i/\partial j + \partial U_j/\partial i)$ is the deformation tensor. The average of the phase factor in equation (21) may be evaluated by noticing that the phase shift $\Delta\Phi_n$ is the sum over a large number n of scattering events. It then follows from the central limit theorem that $\Delta\Phi_n$ is a random Gaussian variable, giving:

$$\begin{aligned}< \exp(j\Delta\Phi_n) > &= \exp(j < \Delta\Phi_n >) \\ &\quad \cdot \exp\left(-\frac{<\Delta\Phi_n^2> - <\Delta\Phi_n>^2}{2}\right)\end{aligned} \tag{22}$$

and then

$$|g_E(t_1, t_2)| = \sum_{n=1}^{\infty} P(n) \exp\left(-\frac{<\Delta\Phi_n^2> - <\Delta\Phi_n>^2}{2}\right) \tag{23}$$

The fluctuations of the phase shift of the light may be computed by properly averaging the phase shift over all the possible orientations of the scattering vectors [16, 17]:

$$\begin{aligned}&< \Delta\Phi_n^2 > - < \Delta\Phi_n >^2 = \\ &\frac{2}{15} n k^2 l^2 \left(\frac{l^*}{l}\right) \left(\left(\sum_i U_{ii}\right)^2 + 2. \sum U_{ij}^2\right)\end{aligned} \tag{24}$$

If the deformation tensor is not homogeneous in the granular material, the quantity U_{ij} should be understood as a component of the tensor properly averaged over the cloud of light paths [17]. We have introduced in equation (24) the scattering mean free path $l =< l_\nu >$. For a dense packing of beads, we expect this distance to be roughly the diameter of the beads. The quantity l^* is the transport mean free path of the light [12]. Since few scattering events are needed in order to randomize the orientation of an optical ray in the granular medium, we expect l^*/l to be a few units. It is then more convenient to consider the length s of a random walk of a photon in the granular medium involving n scattering events. This walk may be viewed as composed of $n^* = nl/l^*$ independent steps of length l^*. Thus from equations (23) and (24), we may express $|g_E(t_1, t_2)|$ as:

$$|g_E(t_1, t_2)| = \sum_s P(s). \exp\left(-k^2 s l^* f(\mathbf{U}(t_1, t_2))\right) \tag{25}$$

with

$$f(\mathbf{U}(t_1, t_2)) = \frac{1}{15}\left(\left(\sum_i U_{ii}\right)^2 + 2. \sum_{i,j} U_{ij}^2\right) \tag{26}$$

where $P(s)$ is the path length distribution through the sample. This quantity depends on the geometry of the experiment, and may be obtained by solving the diffusion equation with boundary conditions corresponding to the geometry of the experiment [14]. The first geometry we used was a slab of thickness L illuminated with a plane wave. The scattered light is collected on the opposite face. The corresponding autocorrelation function is then:

$$|g_E^{(t)}| \approx \frac{kL\sqrt{3f(\mathbf{U})}}{\sinh(kL\sqrt{3f(\mathbf{U})})} \tag{27}$$

We also used the backscattering geometry where the scattered light is collected on the side that is illuminated. In this case, for a slab of infinite thickness, the autocorrelation function is:

$$|g_E^{(r)}| \approx \exp^{-2kl^*\sqrt{3f(\mathbf{U})}} \tag{28}$$

and we take into account, if necessary, the corrections arising from the finite thicknesses of slabs.

4 Thermal expansion of a granular material

In the preceeding section, we derived in equations (27) and (28) the relationship between the displacement field of the beads and the autocorrelation function of the scattered electric field. We present an experimental test of such behaviour. The typical gradients of displacement fields measured with this technique are, according to equations (27) and (26), of the order of $U_{ij} \sim 1/kL \sim 10^{-6} - 10^{-5}$. In order to obtain such displacements in a controllable way, we used the homogeneous expansion of a granular material subjected to slow temperature variations.

Figure 3 shows the evolution of the autocorrelation function g_E, measured in the transmission geometry for a slab of thickness $L = 2$ mm containing spherical soda lime glass beads of diameter d in the range $d = 40 - 63$ μm subjected to thermal variations. In this experiment, the temperature is first kept at a constant value, then slowly increases by a few degrees at a rate of 0.0315 °C/min and then decreases back to its original value. The time origin t_1 is chosen at the beginning of the data acquisition, when the temperature is constant. As long as the temperature remains constant, the correlation function stays close to unity, indicating that the beads do not experience any measurable displacements. When the temperature increases, the correlation function decreases to zero. Returning the temperature to its original value, brings the correlation function back, close to its original value. This indicates that, when the temperature variations are reversed, the motion of the beads is reversed too, bringing the beads back close to their initial positions. It is possible to check that the small reduction in correlation between the beginning and the end of the experiment is mainly due to a small part of

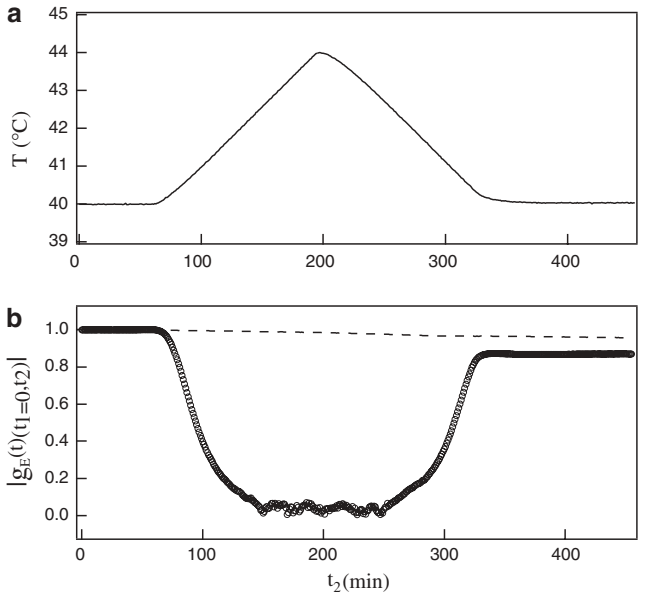

Fig. 3 Response of a granular material to temperature variations. (a) Applied temperature. (b) Symbol: autocorrelation function $|g_E(t_1, t_2)|$ of the scattered electric field measured in a transmission geometry. Dashed line: typical drift of autocorrelation measured when keeping the temperature constant. The time $t_1 = 0$ is chosen to be the time origin

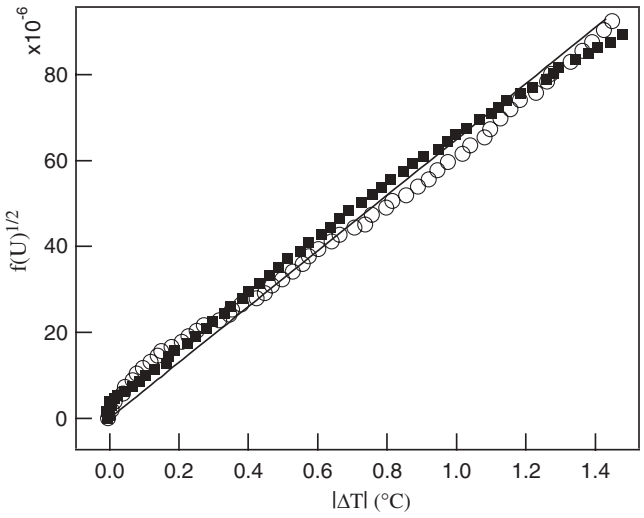

Fig. 4 Mean displacement field extracted from the measurement of the autocorrelation function of the electric field in a transmission (open circles) and a backscattering (full squares) geometry as a function of the temperature variations. Solid line corresponds to $\sqrt{f(\mathbf{U})}$ varying linearly with $|\Delta T|$

irreversible motion during this dilatation-contraction cycle. For this, we performed experiments where we measure the typical drift of the autocorrelation function when the temperature of the granular material is fixed at a constant value. It is found that the correlation remains closer to unity than for the same material undergoing temperature variations, showing that the irreversible motion is mainly due to the dilatation of the granular material. Moreover, we have checked that the same kind of temperature variations applied to a glass frit made of compressed glass beads show that the dilation is perfectly reversible.

We may extract $f(\mathbf{U})$ which is a combination of the components of the deformation tensor $\mathbf{U}$ from the measure of the autocorrelation functions. Figure 4 is a plot of $\sqrt{f(\mathbf{U})}$ as a function of the amplitude of the temperature variations $|\Delta T| = |T(t_1) - T(t_2)|$ for both transmission and backscattering geometries. The value of the transport mean free path l^* is determined to be $l^* = 330\ \mu$m by matching the scale of displacement field values in transmission and in backscattering geometry. This determination is in agreement with the range of values for previous determination of the ratio of the transport mean free path l^* to the bead diameter $d : l^*/d = 6-9$ [4, 18]. As shown on figure 4, the variations of $\sqrt{f(\mathbf{U})}$ are linear with the temperature variations $|\Delta T|$, with a measured slope of 65.10^{-6} K^{-1}. This is in agreement with the fact that we expect the displacement field components to vary linearly with the temperature. We may compare this result with the expected behaviour for an isotropic dilatation of the material, where the deformation field is $U_{ij} = \alpha \Delta T \delta_{ij}$, α being the thermal expansion coefficient. In this case, equation (26) leads to $\sqrt{f(\mathbf{U})} = \alpha|\Delta T|$ which is the observed behaviour. For soda lime glass we expect typical values of the thermal expansion coefficient $\alpha \approx 10.10^{-6}$ K^{-1}, a value significantly lower than the value given by the slope of the figure 4. We may attribute this discrepancy to the simplifying assumptions of simple translations of non deformable spheres. First, the thermal expansion not only displaces the spheres, but dilates them. It follows that the phase variations should be dependant not only on the length of the ray inside each bead, but also on the refractive index variation. Secondly, we did not take into account possible rotations of nonspherical beads. The matter displacement associated with such movement is expected to be of the same order as the simple translation of the beads centers, and to vary linearly with temperature, two features which are indeed observed.

5 Conclusion

We have presented a Diffusing Wave Spectroscopy on a granular material. From measurements of the speckle pattern, we extract the autocorrelation function of the scattered electric field. The loss of correlations may be related to an averaged value of the displacement field of the beads within the material. This technique has been applied to the measurement of the thermal expansion of a granular medium. The displacement field appears to vary linearly with the temperature variations as expected. We restrict this paper to the study of nearly reversible motion. Indeed, obtaining elastic behaviour for granular material, even at relative deformation as small as 10^{-6} is not an easy task. We have mentioned that figure 3 shows that reorganizations occur between initial and final states. It appears during those experiments, that this plastic behaviour clearly depends on various parameters such

as the cohesive forces, the geometrical or mechanical constraints, and the preparation or history of the granular material. Diffusing Wave Spectroscopy appears to be a useful tool for addressing such problems.

Acknowledgements We thank V.Viasnoff and L.Vanel for discussions, and Jeanne Crassous for careful reading of the manuscript.

References

1. De Gennes, P.G.: Reflections on the mechanics of granular matter. Physica A **261**(3–4):267–293 (1998)
2. Pouliquen, O., Chevoir, F.: Dense flows of dry granular material. Computes Rendus Physique **3**(2):163–175 (2002)
3. Komatsu, T.S., Inagaki, S., Nakagawa, N., Nasuno, S.: Creep motion in a granular pile exhibiting steady surface flow. Phys. Rev. Lett. **86**(9):1757–1760 (2001)
4. Menon, N., Durian, D.J.: Diffusing-wave spectroscopy of dynamics in a three-dimensional granular flow. Science **275**(5308):1920–1922 (1997)
5. Menon, N., Durian, D.J.: Particle motions in a gas-fluidized bed of sand. Phys. Rev. Lett. **79**(18):3407–3410 (1997)
6. Kim, K., Park, J.J., Moon, J.K., Kim, H.K., Pak, H.K.,: Solid-liquid transition in a highly dense 3D vibro-fluidized granular system. J. Korean Phys. Soc. Phys. Soc. **40**(6):983–986 (2002)
7. Kabla, A., Debrgeas, G.: Contact dynamics in a gently vibrated granular pile. Phys. Rev. Lett. **92**(3):035501 (2004)
8. Viasnoff, V., Lequeux, F., Pine, D.J.: Multispeckle diffusing-wave spectroscopy: a tool to study slow relaxation and time-dependent dynamics. Rev. Sci. Instr. **73**(6):2336–2334 (2002)
9. Cipelletti, L., Weitz, D.A.: Ultralow-angle dynamic light scattering with a charge coupled device camera based multispeckle, multitau correlator. Rev. Sci. Instr. **70**(8):3214–3221 (1999)
10. Schatzel, K., Schulzdubois, E.O.: Improvements of photon-correlation techniques. Infrared Physics **32**:409–416 (1991)
11. Berne, B.J., Pecora, R.: Dynamic Light Scattering: With Applications to Chemistry, Biology, and Physics, Wiley, New York, (1976)
12. Ishimaru, A.: Wave Propagation and scattering in random media, Academic Press, New York, (1978)
13. Maret, G., Wolf, P.E.: Multiple light scattering from disordered media. The effect of Brownian motion of scatterers. Zeitschrift fur Physik B **65**(4):409–413 (1987)
14. Pine, D.J., Weitz, D.A., Zhu, J.X., Herbolzheimer, E.: Diffusing-wave spectroscopy: dynamic light scattering in the multiple scattering limit. J. Phys. **51**(18):2101–2127 (1990)
15. Bicout, D., Akkermans, E., Maynard, R.: Dynamical correlations for multiple light scattering in laminar flow. J. Phys. I **1**(4):471–491 (1991)
16. Bicout, D., Maynard, R.: Diffusing wave spectroscopy in inhomogeneous flows. Physica A **199**(3–4):387–411 (1993)
17. Bicout, D., Maret, G.: Multiple light scattering in Taylor-Couette flow. Physica A **210**(1–2):87–112 (1994)
18. Leutz, W., Ricka, J.: On light propagation through glass bead packings. Opt. Comm. **126**(4–6):260–268 (1996)